crystals

MDPI

Communication

Nanohardness Measurements of $CdSiP_2$ and $ZnGeP_2$ Chalcopyrite-Type Nonlinear Optical Crystals

Ginka Exner [1], Aleksandar Grigorov [1], Elizabeth Ivanova [1], Peter Schunemann [2], Vladimir Tassev [3], Kevin Zawilski [2] and Valentin Petrov [4,*]

[1] Department of Physics, Faculty of Physics and Technology, Plovdiv University Paisii Hilendarski, 4000 Plovdiv, Bulgaria
[2] BAE Systems, P.O. Box 868, MER15-1813, Nashua, NH 03061, USA
[3] Air Force Research Laboratory (AFRL), Wright-Patterson AFB, Dayton, OH 45433, USA
[4] Max Born Institute for Nonlinear Optics and Ultrafast Spectroscopy, Max-Born-Str. 2a, 12489 Berlin, Germany
* Correspondence: petrov@mbi-berlin.de

Abstract: We study the nanohardness and Young's modulus of randomly oriented $CdSiP_2$ (CSP) and $ZnGeP_2$ (ZGP) single crystals, grown via the horizontal Bridgman method. CSP and ZGP are the only two pnictide chalcopyrites widely used as nonlinear optical crystals in the mid-IR part of the spectrum. Nanoindentation is employed in the continuous stiffness mode (45 Hz, 2 nm) using a Berkovich tip. Nanohardness values of 9.9 ± 0.2 GPa (Knoop hardness of 905 kg/mm^2) for CSP and 11.5 ± 0.1 GPa (993 kg/mm^2) for ZGP are derived. For Young's modulus, we obtain 136 ± 2 GPa (CSP) and 150 ± 2 GPa (ZGP). The trend of increasing hardness with bandgap and melting point of the isostructural CSP and ZGP, as deduced from previous measurements, is not confirmed. The results for ZGP are compared to 2GaP, its binary isoelectronic analog, and the values obtained, 11.0 ± 0.3 GPa for the nanohardness and 154 ± 2 GPa for Young's modulus, indicate good matching within the accuracy limits.

Keywords: nanoindentation; hardness; chalcopyrites; $CdSiP_2$; $ZnGeP_2$; GaP; nonlinear crystals

check for updates

Citation: Exner, G.; Grigorov, A.; Ivanova, E.; Schunemann, P.; Tassev, V.; Zawilski, K.; Petrov, V. Nanohardness Measurements of $CdSiP_2$ and $ZnGeP_2$ Chalcopyrite-Type Nonlinear Optical Crystals. *Crystals* **2023**, *13*, 1164. https://doi.org/10.3390/cryst13081164

Academic Editors: Alessandro Chiasera and Jeroen Beeckman

Received: 1 July 2023
Revised: 18 July 2023
Accepted: 24 July 2023
Published: 26 July 2023

Copyright: © 2023 by the authors. Licensee MDPI, Basel, Switzerland. This article is an open access article distributed under the terms and conditions of the Creative Commons Attribution (CC BY) license (https://creativecommons.org/licenses/by/4.0/).

1. Introduction

$CdSiP_2$ (CSP) and $ZnGeP_2$ (ZGP) are the only two pnictide chalcopyrites belonging to the II-IV-V_2 ternary semiconductors that are commercially available and widely used as non-oxide nonlinear optical crystals in the mid-IR part of the spectrum [1]. Due to their chemical stability and high figure-of-merit, thermal conductivity, and optical damage threshold, they have become the materials of choice for the frequency down conversion of laser radiation from the 1 μm (Nd- and Yb-lasers) and 2 μm (Tm- and Ho-lasers) spectral ranges to longer wavelengths in the mid-IR or THz range. The optical and physical properties of CSP and ZGP including transmission, dispersion, birefringence, second-order nonlinear susceptibility, thermo-optic coefficients, thermal conductivity and expansion, etc., have already been well characterized with respect to potential applications in frequency conversion. However, the actual device implementation also depends to some extent on their mechanical performance. The mechanical properties are important since the technical design demands appropriate cutting and polishing procedures, as well as subsequent cleaning and anti-reflection coating of the optical surfaces. During operation, thermal and mechanical stresses often occur, related to residual (unwanted) absorption at high average powers. Hence, a priori knowledge of their durability, i.e., an estimation of thermal stress effects of these nonlinear optical materials, concerning the technological processes and behavior during the device exploitation, is a prerequisite for their subsequent successful application.

From a fundamental point of view, mechanical properties are an essential part of material characterization. They are closely related to and determined by the interatomic

interactions, the material density, the optical bandgap, the melting point, etc. The old literature data on these two compounds, specified as Knoop microhardness, provide scattered values in the range of 744–1050 kg/mm^2 for CSP [2,3] and 620–980 kg/mm^2 for ZGP [3–6], with a trend of higher hardness for the compound possessing a wider bandgap and higher melting point [3], i.e., CSP. Because of the stronger dependence on material quality of the measured optical bandgaps, e.g., the presence of near-bandgap defect-related absorption, it is more reliable to correlate hardness results with the melting points of 1133 °C for CSP and 1027 °C for ZGP [7]. The main problem with such old data is that in many cases polycrystalline samples were used, and the exact measuring techniques were not specified or different equipment and settings were employed, meaning that a reasonable comparison of the results is hard to be considered reliable. A data comparison is also complicated because ZGP has been in use in nonlinear optics since the early 1970s, while CSP was introduced roughly four decades later. In most cases, the origin of the data can be traced back to one review [5] and two books in Russian [3,8]. Neumann has compiled these data in GPa units, including error limits [9].

In general, the mechanical properties of such ternary chalcopyrites can be compared with their binary isoelectronic (compounds with the same number of valence electrons) analogs. In the present study, nanohardness and Young's modulus are experimentally measured by means of nanoindentation using single crystalline polished samples of CSP and ZGP of similar quality, which enables unambiguous comparison. The results for ZGP are also compared to its closest isoelectronic analog, GaP (with both possessing 16 valence electrons).

2. Materials and Methods

CSP and ZGP belong to the tetragonal $I\bar{4}2d$ space group (point group $\bar{4}2m$), i.e., they are non-centrosymmetric and anisotropic crystals. Both of them were grown using the horizontal gradient freeze (HGF) technique, which is a modification of the classical Bridgman method [10–12]. Polycrystalline charges were synthesized from stoichiometric amounts of high-purity (>99.9999%) Cd, Si, Zn, Ge, and red P starting materials. This ensured the high quality (purity and structure) of the obtained single crystals, which is of paramount importance for the mechanical properties. The binary isoelectronic analog of CSP is InP + AlP and that of ZGP is 2GaP (where 2 stands for two lattice unit cells equivalent to one of ZGP) [3,5]. Thus, only the latter one exists as a single crystal in a sufficiently large thickness for comparative measurements. The binary III-V counterparts of the II-IV-V_2 semiconductors exhibit a zinc-blende structure and are also non-centrosymmetric (space group $F\bar{4}3m$, point group $\bar{4}3m$), but they are optically isotropic (cubic). The melting point of GaP is 1457 °C. The GaP sample used here was grown on a commercial-grade (100) GaAs wafer in a horizontal quartz reactor under low pressure (<1.3 kPa) via hydride vapor phase epitaxy (HVPE) [13]. Prior to the measurements, the substrate was removed entirely.

The 2.2 mm thick CSP and ZGP plates used for the hardness and Young's modulus measurements were the same as those previously employed for the estimation of the optical damage threshold [14]. These samples were double-side polished to laser quality, as described elsewhere [15]. Hybrid mechanical–chemical polishing was applied to the epitaxial GaP layer (Impex HighTech, Münster, Germany) and the resulting thickness amounted to 204 μm (as measured via interference fringes).

In the present study, nanoindentation was employed as a modern technique to study the mechanical behavior of the crystals in terms of hardness and Young's modulus. In nanoindentation tests, pressing a hard indenter with a specific geometry into the sample surface causes penetration into the sample volume. The indentation tip leaves a small-size residual impression, as a result of elastic and plastic deformations. Hardness is then described as the resistance to plastic deformation during the constant load from the sharp indenter. It is then derived as the load per unit area of indentation. The nanoindentation is advantageous compared to established microhardness tests, especially when brittle materials as the semiconductor crystals are to be investigated. It requires only small-size

samples and offers precise control over the load. Another advantage of nanoindentation is that the indentation depth, instead of the area (estimated from microscopy images), is used to evaluate the physical quantities, which improves the precision of the derived values. Young's modulus, E, is a fundamental physical quantity, describing the proportionality of the stress, σ, versus strain, ε, for a material undergoing elastic deformation: $\sigma = E\varepsilon$.

G200 Nanoindenter equipment (Keysight Technologies, Santa Rosa, CA, USA) was employed in the present study. The continuous stiffness mode (CSM) was chosen, which allows one to evaluate the hardness and Young's modulus versus the penetration depth. Here, small oscillations, giving a depth of 2 nm, are superimposed onto the main load. This way, partial relaxation of the structure takes place, decreasing the probability of inducing cracks and breaking the samples. The oscillation frequency was fixed to 45 Hz for all measurements. Special care was taken to equilibrate both the equipment tip and the samples, since this can affect the final results by causing unacceptable displacement due to thermal expansion or contraction of the equipment or sample at the contact between them during the test. This was achieved by the option "thermal drift correction" of the equipment. As a reference material, polished fused silica was used, for which values of 71.3 ± 0.6 GPa for Young's modulus and 9.5 ± 0.1 GPa for the hardness were obtained. They fit into the device acceptance criteria (70–75 GPa and 8.5–10.5 GPa, respectively).

In the present experiments, the total indentation depth amounted to 2000 nm and the strain rate to the target was constant with a value of 0.05 s^{-1}. The surface approach velocity was 10 nm/s and the surface approach distance was selected to be 1 µm. The chosen parameters enable an exact location of the sample surface, which is then taken as the zero of the displacement into surface coordinate. It should be emphasized that an incorrectly found surface will make the accurate determination of hardness and Young's modulus impossible. Luckily, this could be considered as an advantage as well, since such tests were automatically discarded by the software and they did not contribute to the statistical estimation of the monitored parameters. The nanoindentation was conducted using a Berkovich tip, having a nominal tip radius of about 50 nm (tip bluntness).

In CSM, the hardness and Young's modulus are estimated at each oscillatory step during partial unloading, so that the depth dependence of both quantities can be obtained. The data were collected and processed via the *NanoSuite 6* Software of the nanoindenter equipment.

The room temperature was held constant (23 °C ± 1 °C), and the relative humidity was about 43%. For the tests, the samples were attached to a specially designed holder (disc) with a 50 °C flow point "crystal bond" adhesive (Figure 1a). Prior to the measurement, the surface was cleaned with acetone and the sample was left to cool down to room temperature.

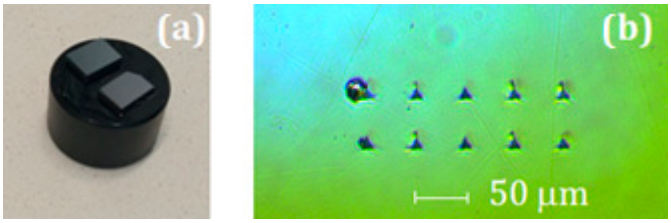


Figure 1. (**a**) ZGP (upper left) and CSP (lower right) samples glued on the holder; (**b**) representative view of the 10 indents (CSP sample).

Ten consecutive indents were performed in each case, where the spots were ordered in two rows, and the distance between the adjacent spots was 50 µm (Figure 1b). This spacing was chosen to ensure independent indents, which should be separated by a distance between 20 and 30 times the maximum depth of the indentation. In our case, the separation was 25 times the depth of 2000 nm. A slight sink-in effect on the residual impression of the Berkovich diamond indenter was observed, but the Oliver–Pharr approach [16] for elastic moduli estimation was still justified.

The hardness, H_{IT}, was calculated as follows:

$$H_{IT} = P/A \quad (1)$$

where P is the contact force and A is the contact area.

Young's modulus, E_{IT}, was calculated, taking into account Young's modulus of the indenter, E_i, and the reduced elastic modulus of the sample, E_r:

$$E_{IT} = \left(1 - \nu^2\right)\sqrt{1/E_r - \left(1 - \nu_i^2\right)/E_i} \quad (2)$$

where ν is Poisson's ratio (in this case taken as 0.2, following the manual) and E_r equals the following:

$$E_r = \left(\sqrt{\pi}\, S\right)/\left(2\beta\sqrt{A}\right) \quad (3)$$

Here, S is the contact stiffness (measured at each oscillatory step), A is the surface contact area projected onto a plane normal to the direction of indentation, and β is a geometrical factor depending on the indenter (for a Berkovich tip it equals 1.034).

3. Results and Discussion

Figure 2 shows the loading and unloading curves for the investigated crystals. As can be seen, the higher load, in order to achieve the maximum depth, was exerted for ZGP (about 588 mN), whereas it was about 510 mN for CSP. Based on the loading curves, the nanohardness, H_{IT}, and Young's modulus, E_{IT}, were evaluated. The curves are free from pop-in effects (sudden increase in the indentation depth). Pop-in effects depend on crystal defects (such as homogeneous nucleation during the load; pinned dislocations, whose motion is unlocked; movement and multiplication of preexisting dislocations; etc.) and their density. Hence, a lack of such effects is evidence of excellent crystal quality.

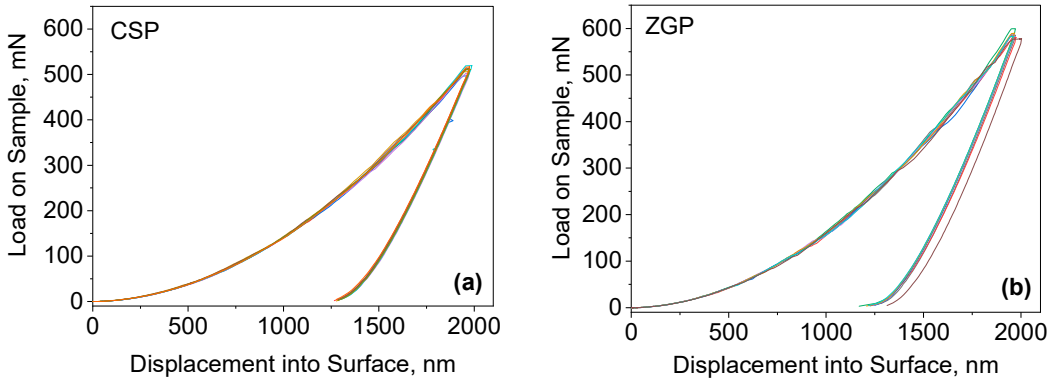


Figure 2. Loading and unloading curves for (**a**) CSP and (**b**) ZGP. Each test is given in a different color.

In Figure 3, the results for the nanohardness and Young's modulus of CSP are shown. As can be seen, all of the tests overlap quite well, showing good reproducibility at depths above about 300 nm. The difference close to the surface might originate from surface scratches or some other imperfections. Hence, the average values for both quantities were taken in the range from 300 to 1800 nm. Table 1 includes the obtained average values together with some experimental details. The results can be converted to Knoop or Vickers hardness, so that the values correspond to 905 (Knoop) and 918 kg/mm^2 (Vickers, VHN (kg/mm^2) = 92.7 H (GPa)).

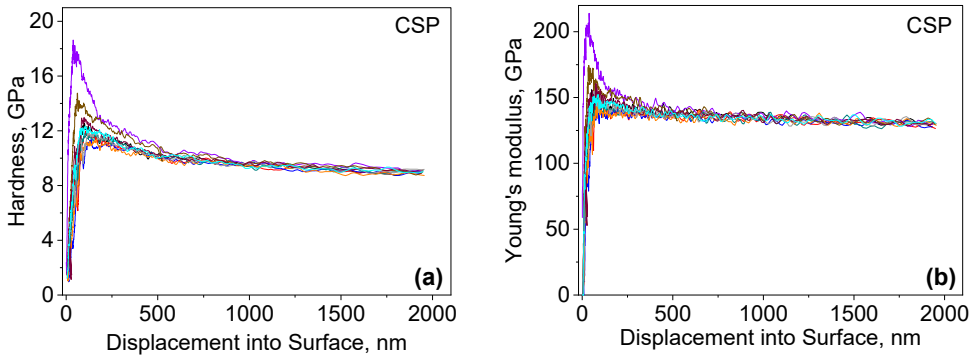


Figure 3. CSP depth dependence of (**a**) nanohardness and (**b**) Young's modulus. Each test is given in a different color.

Table 1. Nanohardness and Young's modulus, sample temperature, and drift correction. The nanohardness (Knoop) in kg/mm^2 is calculated from the average values in GPa.

	Nanohardness GPa	**Nanohardness Knoop, kg/mm^2**	**Young's Modulus GPa**	**Temperature °C**	**Drift Correction nm/s**
CSP	9.9 ± 0.2	905	136 ± 2	23.7 ± 0.2	0.27 ± 0.01
ZGP	11.5 ± 0.1	993	150 ± 2	24.2 ± 0.1	0.25 ± 0.01
2GaP	11.0 ± 0.3	967	154 ± 2	23.0 ± 0.2	0.44 ± 0.04

In Figure 4, the results for the nanohardness and Young's modulus of ZGP are shown. Similarly to the previous case, all of the tests overlap quite well, except in the initial range up to about 300 nm. The average values for both quantities, taken in the range from 300 to 1800 nm, are given in Table 1. The results can be converted into Knoop or Vickers hardness, yielding values of 993 (Knoop) and 1066 kg/mm^2 (Vickers).

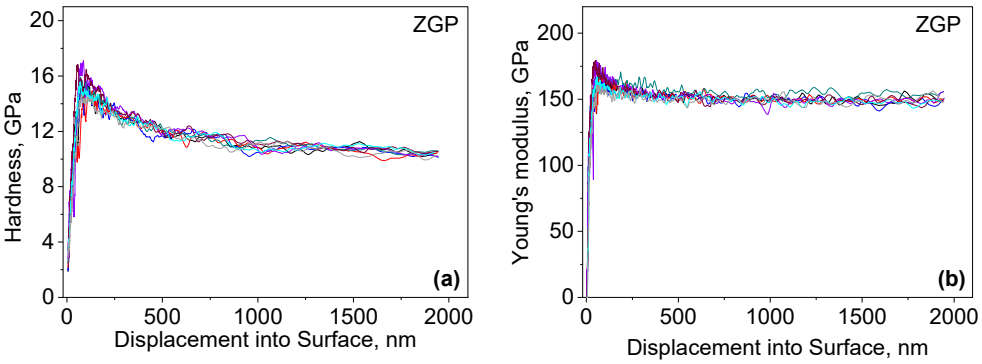


Figure 4. ZGP depth dependence of (**a**) nanohardness and (**b**) Young's modulus. Each test is given in a different color.

Our results indicate that the hardness and Young's modulus of ZGP are higher compared to CSP, in contradiction with the general trend mentioned in the introductory part. Some models indeed predict higher hardness of ZGP compared to CSP. Since the strength of the cohesive forces defines the compressibility, hardness, and melting point of a crystal, i.e., stronger cohesive forces imply more resistance to compression, to indentation, and to thermal atomic motion, in [2], the hardness is related to the Debye temperature ($\theta = h \cdot \nu_m / k_B$, where h is Planck's constant, k is Boltzmann's constant, and ν_m is the maximum lattice vibration frequency). Indeed, the calculated Debye temperature is 314 K for ZGP and 274 K for CSP [2], supporting our results. Neumann [9] proposed a simple relationship between the unit cell volume V_0 and the ratio of the hardness H versus melting temperature T_m, measured in K, with two fitting parameters which are almost constant for the pnictide-type

chalcopyrites. The dependence of decreasing H/T_m with V_0 is confirmed by our results via the two representatives of this family, CSP and ZGP, although the predicted H values are nearly the same. If the exact values of the average bond ionicities, tabulated in [9], are taken into account in this model, it follows, however, that the compound with larger iconicity (CSP) must at least qualitatively exhibit lower hardness. The same trend, as observed experimentally by us, was also predicted by the plasma oscillation theory of solids [17], although the relationship suggested by these authors contradicted previously reported experimental microhardness values cited in their paper, which have now turned out to be inaccurate.

The load at the maximum depth for 2GaP was about 558 mN, which is lower than that of its ternary equivalent ZGP. The hardness and Young's modulus depth dependences are shown in Figure 5 and the average values for the same range as for the ternary crystals are listed in Table 1. The results show that both the hardness and Young's modulus of 2GaP match well the values for ZGP within the accuracy limits. This corresponds to almost equal bandgaps, although the melting temperature of the binary analog is much higher [5]. Our results for GaP are close to the experimental microhardness value of 940 kg/mm^2 from [5] and also confirm more recent nanoindentation tests [18], giving 10.9 ± 0.2 GPa for the hardness and 147 ± 5 GPa for Young's modulus of GaP.

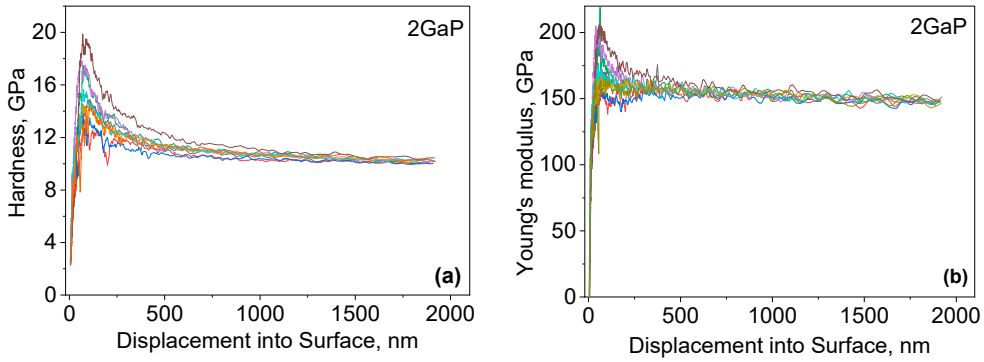


Figure 5. 2GaP depth dependence of (**a**) nanohardness and (**b**) Young's modulus. Each test is given in a different color.

In fact, the plasma oscillation theory of solids failed to correctly predict the hardness of GaP. Hence, the specific interactions seem to be of primary importance for the mechanical response. They are obviously different in the case of ZGP and CSP. Some hint of this is, for instance, their thermal behavior. The thermal expansion of CSP differs by about a factor of four along and perpendicular to the *c*-axis and the signs are different (anomalous expansion), while ZGP is far less anisotropic with only about 50% larger thermal expansion perpendicular to the *c*-axis. Thus, comparative studies with different orientations could be performed in the future. Interestingly, some other related properties also show an unexpected trend, e.g., the optical damage threshold of ZGP is higher compared to CSP [14].

4. Conclusions

Nanohardness and Young's modulus of two ternary chalcopyrites, $CdSiP_2$ and $ZnGeP_2$, were obtained via nanoindentation. Nanohardness of 9.9 ± 0.2 GPa and Young's modulus of 136 ± 2 GPa were obtained for CSP, and 11.5 ± 0.1 GPa and 150 ± 2 GPa were obtained for ZGP, respectively. The results contradict the expected trend of increasing values with melting temperature and bandgap, but support some previously developed empirical models. At present, we have to assume that this is only a deviation for these two compounds, but the general trend seems to hold for all other chalcopyrite crystals; see, e.g., [7].

The comparison with GaP as the binary isoelectronic analog of ZGP shows a remarkable match of the two quantities, with 11.0 ± 0.3 GPa for the nanohardness and 154 ± 2 GPa for Young's modulus. Since the plasma oscillation theory failed to predict such values, the overall results have to also be considered in terms of the specificity of the interatomic interactions in each of the crystals.

Author Contributions: Conceptualization, V.P.; methodology, V.P., P.S., V.T. and G.E.; formal analysis, A.G. and E.I.; investigation, G.E., A.G. and E.I.; resources, K.Z., P.S. and V.T.; data curation, A.G., G.E. and E.I.; writing—original draft preparation, G.E. and V.P.; writing—review and editing, V.P. and P.S.; visualization, A.G., G.E. and E.I.; supervision, V.P.; funding acquisition, V.P. All authors have read and agreed to the published version of the manuscript.

Funding: This research has been supported by the Air Force Office of Scientific Research, award # FA8655-20-1-7053.

Data Availability Statement: Data are available from the corresponding author upon reasonable request.

Acknowledgments: The authors acknowledge the project BG05M20P001-1.002-0005, Personalized Innovative Medicine Competence Center (PERIMED) for providing the equipment used in this research.

Conflicts of Interest: The authors declare no conflict of interest. The funders had no role in the design of the study; in the collection, analyses, or interpretation of data; in the writing of the manuscript; or in the decision to publish the results.

References

1. Petrov, V. Frequency down-conversion of solid-state laser sources to the mid-infrared spectral range using non-oxide nonlinear crystals. *Prog. Quantum Electron.* **2015**, *42*, 1–106. [CrossRef]
2. Abrahams, S.C.; Hsu, F.S.L. Debye temperatures and cohesive properties. *J. Chem. Phys.* **1975**, *63*, 1162–1165. [CrossRef]
3. Goryunova, N.A. *Complex Diamond-like Semiconductors*; Sovetskoe Radio: Moscow, Russia, 1968. (In Russian)
4. Shay, J.L.; Wernick, J.H. *Ternary Chalcopyrite Semiconductors: Growth, Electronic Properties, and Applications*; Pergamon Press: Oxford, UK, 1975.
5. Borshchevskii, A.S.; Goryunova, N.A.; Kesamanly, F.P.; Nasledov, D.N. Semiconducting $A^{II}B^{IV}C_2^V$ compounds. *Phys. Stat. Sol.* **1967**, *21*, 9–55. [CrossRef]
6. Yao, G.-Q.; Shen, H.-S.; Kershaw, R.; Dwight, K.; Wold, A. Peparation and characterization of $ZnSiP_2$ and $ZnGeP_2$ single crystals. *Mater. Res. Bull.* **1986**, *21*, 653–660. [CrossRef]
7. Schunemann, P.G.; Zawilski, K.T. New ternary chalcopyrite semiconductors for mid-IR NLO frequency conversion. In *SPIE Proceedings PC12405: Nonlinear Frequency Generation and Conversion: Materials and Devices XXII, PC124050J*; SPIE: Bellingham, WA, USA, 2023. [CrossRef]
8. Goryunova, N.A.; Valov, Y.A. (Eds.) $A^2B^4C_2^5$ *Semiconductors*; Sovetskoe Radio: Moscow, Russia, 1974. (In Russian)
9. Neumann, H. Microhardness scaling and bulk modulus-microhardness relationship in $A^{II}B^{IV}C_2^V$ chalcopyrite compounds. *Cryst. Res. Technol.* **1988**, *23*, 97–102. [CrossRef]
10. Schunemann, P.G.; Pollak, T.M. Method for Growing Crystals. U.S. Patent 5,611,856, 18 March 1997. Available online: https://patents.google.com/patent/US5611856A/en (accessed on 20 July 2023).
11. Zawilski, K.T.; Schunemann, P.G.; Pollak, T.C.; Zelmon, D.E.; Fernelius, N.C.; Hopkins, F.K. Growth and characterization of large $CdSiP_2$ single crystals. *J. Cryst. Growth* **2010**, *312*, 1127–1132. [CrossRef]
12. Zawilski, K.T.; Schunemann, P.G.; Setzler, S.D.; Pollak, T.M. Large aperture single crystal $ZnGeP_2$ for high-energy applications. *J. Cryst. Growth* **2008**, *310*, 1891–1896. [CrossRef]
13. Tassev, V.; Vangala, S.; Brinegar, D.; Parker, M.; Barlow, T. Thick heteroepitaxy of binary and ternary semiconductor materials for nonlinear frequency conversion in the mid and longwave infrared region. *Phys. Stat. Sol. A* **2021**, *218*, 2000443. [CrossRef]
14. Hildenbrand, A.; Kieleck, C.; Tyazhev, A.; Marchev, G.; Stöppler, G.; Eichhorn, M.; Schunemann, P.G.; Panyutin, V.L.; Petrov, V. Laser damage of the nonlinear crystals $CdSiP_2$ and $ZnGeP_2$ studied with nanosecond pulses at 1064 and 2090 nm. *Opt. Eng.* **2014**, *53*, 122511. [CrossRef]
15. Zawilski, K.T.; Setzler, S.D.; Schunemann, P.G.; Pollak, T.M. Increasing the laser-induced damage threshold of single-crystal $ZnGeP_2$. *J. Opt. Soc. Am. B* **2006**, *23*, 2310–2316. [CrossRef]
16. Oliver, W.C.; Pharr, G.M. An improved technique for determining hardness and elastic modulus using load and displacement sensing indentation experiments. *J. Mater. Res.* **1992**, *7*, 1564–1583. [CrossRef]
17. Kumar, V.; Shrivastava, A.K.; Jha, V. Bulk modulus and microhardness of tetrahedral semiconductors. *J. Phys. Chem. Solids* **2010**, *71*, 1513–1520. [CrossRef]
18. Grillo, S.E.; Ducarroir, M.; Nadal, M.; Tourni, E.; Faurie, J.-P. Nanoindentation of Si, GaP, GaAs and ZnSe single crystals. *J. Phys. D Appl. Phys.* **2003**, *36*, L5–L9. [CrossRef]

Disclaimer/Publisher's Note: The statements, opinions and data contained in all publications are solely those of the individual author(s) and contributor(s) and not of MDPI and/or the editor(s). MDPI and/or the editor(s) disclaim responsibility for any injury to people or property resulting from any ideas, methods, instructions or products referred to in the content.